

Identification and Quantitation of Neutrophil Extracellular Traps in Human Tissue Sections

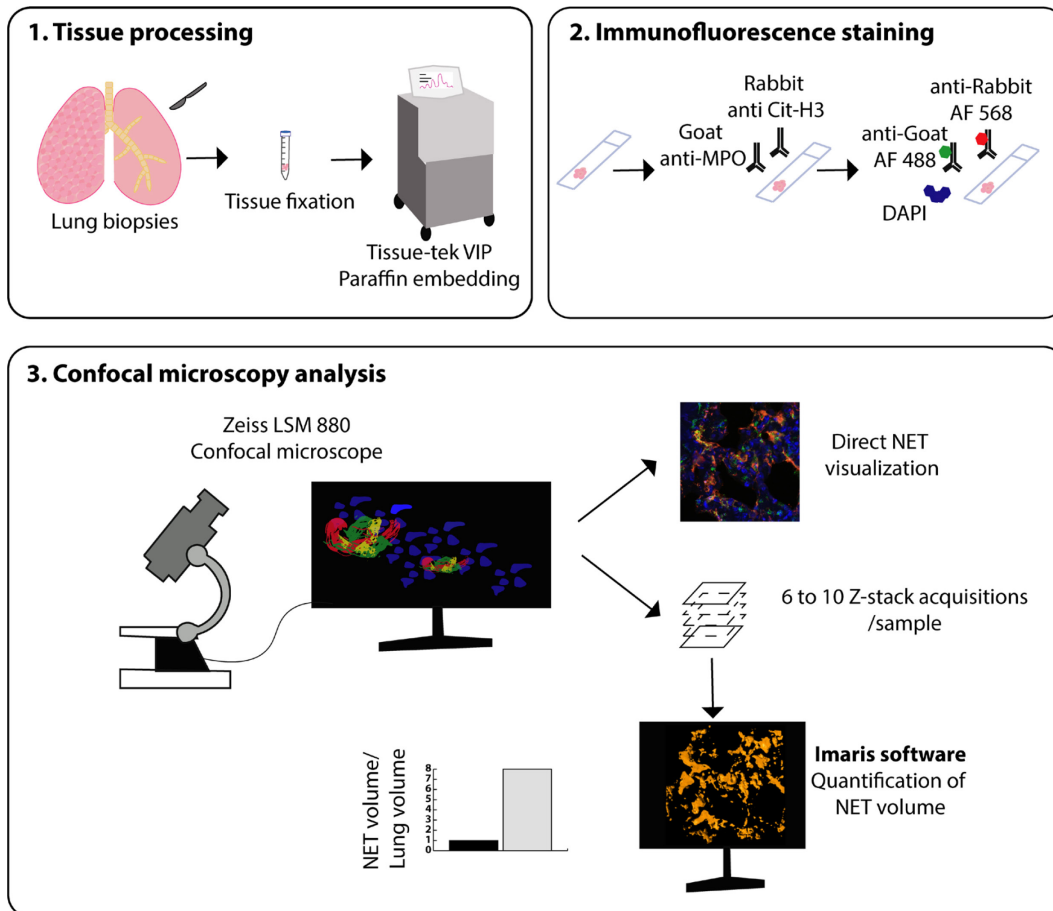
Coraline Radermecker^{1,2}, Alexandre Hego³, Philippe Delvenne^{4,5} and Thomas Marichal^{1,2,*}

¹Laboratory of Immunophysiology, Grappe Interdisciplinaire de Genoproteomique Appliquee (GIGA) Institute, Liege University, Liege, Belgium; ²Faculty of Veterinary Medicine, Liege University, Liege, Belgium; ³Cell Imaging platform, Grappe Interdisciplinaire de Genoproteomique Appliquee (GIGA), Liege, Belgium; ⁴Department of Pathology, Clinique Hospitalo-Universitaire (CHU) University Hospital, Liege University, Liege, Belgium; ⁵Laboratory of Experimental Pathology, Grappe Interdisciplinaire de Genoproteomique Appliquee (GIGA) Institute, Liege University, Liege, Belgium

*For correspondence: t.marichal@uliege.be

[Abstract] Neutrophils are one of the first innate immune cells recruited to tissues during inflammation. An important function of neutrophils relies on their ability to release extracellular structures, known as Neutrophil Extracellular Traps or NETs, into their environment. Detecting such NETs in humans has often proven challenging for both biological fluids and tissues; however, this can be achieved by quantitating NET components (*e.g.*, DNA or granule/histone proteins) or by directly visualizing them by microscopy, respectively. Direct visualization by confocal microscopy is preferably performed on formalin-fixed paraffin-embedded (FFPE) tissue sections stained with a fluorescent DNA dye and antibodies directed against myeloperoxidase (MPO) and citrullinated histone 3 (Cit-H3), two components of NETs, following paraffin removal, antigen retrieval, and permeabilization. NETs are defined as extracellular structures that stain double-positive for MPO and Cit-H3. Here, we propose a novel software-based objective method for NET volume quantitation in tissue sections based on the measurement of the volume of structures exhibiting co-localization of Cit-H3 and MPO outside the cell. Such a technique not only allows the unambiguous identification of NETs in tissue sections but also their quantitation and relationship with surrounding tissues.

Graphic abstract:



Graphical representation of the methodology used to stain and quantitate NETs in human lung tissue.

Keywords: Neutrophil, Neutrophil extracellular traps, Lung, Tissue sections, Confocal microscopy, NET quantitation

[Background] Neutrophils are the major innate immune cells in the blood (50-70% of white blood cells in humans) (Mestas and Hughes, 2004). These cells have a diameter of 5-7 μm and are characterized by a segmented nucleus, secretory vesicles in their cytoplasm, and a short lifespan (Borregaard, 2010). Neutrophils are produced in the bone marrow in response to G-CSF secretion under the control of key transcription factors such as PU.1, C/EBP α , GFI-1, and C/EBP ϵ (Hidalgo *et al.*, 2019). Neutrophils participate in pathogen destruction by releasing the cytotoxic contents of their secretory vesicles or by phagocytosis (Borregaard, 2010). Recently, several discoveries have shed light on neutrophil biology and function. First, a study using radiolabeling of neutrophils demonstrated an unexpected longer half-life of these cells, which can reach 5.4 days in humans and 18 hours in mice (Pillay *et al.*, 2010). Second, in 2004, Brinkmann and colleagues discovered a novel bactericidal action of neutrophils. Indeed, it was observed that the release of particular structures could trap bacteria and limit their dissemination throughout the organism (Brinkmann *et al.*, 2004). These new structures were named Neutrophil Extracellular Traps or NETs. NETs are web-like structures composed of extracellular free DNA

associated with a particular form of citrullinated histone 3 (Cit-H3), in which arginine residues have been replaced by citrulline, and various antimicrobial peptides from secretory vesicles, such as myeloperoxidase (MPO), neutrophil elastase (NE), or cathelicidins (Papayannopoulos, 2018). The release of these structures can be triggered by various stimuli derived from bacteria, viruses, parasites, and fungi, but also by immune complexes, crystals, pro-inflammatory cytokines, and chemokines (Papayannopoulos, 2018). Within neutrophils, the activation of pyruvate kinase C, formation of reactive oxygen species (ROS), and the activation of peptidyl arginase 4 and neutrophil elastase allow chromatin decondensation, nuclear membrane disruption, and NET release (Papayannopoulos, 2018). NETs can immobilize pathogens and prevent their dissemination but are also able to kill them directly (Brinkmann *et al.*, 2004; Papayannopoulos, 2018). Unfortunately, excessive NET release or inappropriate NET accumulation can trigger important tissue damage and lesions (Narasaraju *et al.*, 2011) or inadequate activation of immune cells, thereby promoting various immune-mediated disorders (Hakim *et al.*, 2010; Radermecker *et al.*, 2019) or coagulation issues (Middleton *et al.*, 2020). Thus, NETs are increasingly implicated in various pathological processes, as evidenced by experimental work in mouse models (Radermecker *et al.*, 2019; Villanueva *et al.*, 2011). The investigation into their potential contributions to human disease is therefore of great interest. NET detection in humans is quite challenging and can be performed either indirectly in physiological fluids or directly in tissue sections. To date, NETs have been mainly measured in physiological fluids such as serum and bronchoalveolar lavage fluid (BALF) (Toussaint *et al.*, 2017; Middleton *et al.*, 2020). NET measurements in fluids rely on the detection of one or two of their components (extracellular DNA, citrullinated histone 3, or complexes of DNA/MPO or DNA/NE). Extracellular free DNA can be detected using DNA quantitation assays on serum or BALF supernatant (Toussaint *et al.*, 2017). Methods for the detection of Cit-H3 have been developed, including western blotting (Liu *et al.*, 2016; Thålin *et al.*, 2017). A more specific technique relies on the detection of complexes formed by DNA and one of the antimicrobial peptides released from secretory vesicles, like MPO or NE, by ELISA (Caudrillier *et al.*, 2012; Caldarone *et al.*, 2019). These techniques are rapid but lack specificity and do not provide any information about the location of NETs in the tissue. Here, we describe a protocol allowing the direct visualization and quantitation of NETs *in situ* by confocal microscopy. NETs are identified as extracellular structures exhibiting a co-localization of Cit-H3 and MPO, two important components of NETs. This technique is currently considered the gold standard of NET detection. Furthermore, we propose a novel software-based objective method to quantitate NETs in tissues based on the measurement of the volume of structures exhibiting a co-localization of Cit-H3 and MPO outside the cell (Radermecker *et al.*, 2019). This technique is specific, quantitative, and provides information about the location of NETs in tissues (Radermecker *et al.*, 2020). Identification of specific NET-rich areas in human tissues may promote a better understanding of their pathological roles in disease.

Materials and Reagents

1. Coverslips, 22 × 22 mm (Fisher Scientific, ThermoFisher Scientific, catalog number: 15727582)

2. Microscope slides, Superfrost (VWR, catalog number: 631-0113)
3. Pipette tips
4. Bovine serum albumin (Sigma-Aldrich, catalog number: 9048-46-8), stored at 4-8°C
5. Donkey serum (Sigma-Aldrich, catalog number: D9663), stored at -20°C
6. Goat anti-human/mouse myeloperoxidase antibody (Novus Biologicals, catalog number: AF3667), stored at -20°C
7. Rabbit anti-histone H3 (citruiline R2+R8+R17) antibody (Abcam, catalog number: ab5103), stored at -20°C
8. Donkey anti-goat IgG (H+L) highly cross-adsorbed secondary antibody, Alexa Fluor 488-conjugated (ThermoFisher Scientific, catalog number: A32814), stored at 4-8°C
9. Donkey anti-rabbit IgG (H+L) highly cross-adsorbed secondary antibody, Alexa Fluor 568-conjugated (ThermoFisher Scientific, catalog number: A10042), stored at 4-8°C
10. Neo Clear (Sigma-Aldrich, catalog number: 64741-65-7)
11. Absolute ethanol (Fisher Chemical, catalog number: E/0600DF/15)
12. Xylene (VWR, catalog number: 28973.363)
13. Ultrapure DNase/RNase-free distilled water (ThermoFisher Scientific, Invitrogen, catalog number: 10977049)
14. DAPI (Sigma-Aldrich, catalog number: 28718-90-3), stored at -20°C
15. ProLong Gold antifade mountant (ThermoFisher Scientific, catalog number: P10144), stored at -20°C
16. Goat IgG isotype control (ThermoFisher Scientific, catalog number: 31245), stored at 4-8°C
17. Rabbit IgG isotype control (ThermoFisher Scientific, catalog number: 31235), stored at 4-8°C
18. Formaldehyde (Sigma-Aldrich, catalog number: 47608)
19. HIER Tris-EDTA Buffer, pH 9.0 (10×) (Zytomed Systems, catalog number: ZUC029-500), stored at 4-8°C
20. Tween-20 (Fisher Scientific, Acros Organics, catalog number: 10491081), stored at room temperature (RT)
21. Triton X-100 (Sigma-Aldrich, catalog number: 9002-93-1), stored at room temperature (RT)
22. Antigen Retrieval Buffer (see Recipes)
23. Permeabilization Buffer (see Recipes)
24. Blocking Buffer (see Recipes)

Equipment

1. Tissue-Tek-VIP 5 (Sakura)
2. Rotary microtome (Leica)
3. Zeiss LSM 880 Airyscan Elyra s.1. confocal microscope (Zeiss)
4. StainTray slide staining system (Sigma-Aldrich, catalog number: Z670146)

5. Kartell PMPHellendhal staining jar (ThermoFisher Scientific, Fisher Scientific, catalog number: 10375681)
6. Portable steam sterilizer (Prestige Medical, 2100 classic)
7. Pipettes
8. Refrigerator (4°C)
9. Freezer (-20°C)
10. Chemical fume hood

Software

1. ImageJ (version 15.1n, NIH, <https://imagej.nih.gov/ij/download.html>)
2. Imaris (version 7.5.2, oxford instruments)
3. Zen black (Zeiss)

Procedure

A. Sample collection, fixation, and paraffin embedding

1. Collect lung post-mortem biopsies and fix them for three hours at RT in 4% formaldehyde.
 2. After fixation, embed the biopsies in paraffin, following these three steps:
 - a. Dehydration: The fixation agent is eliminated by successive baths of increasing ethanol concentration: three times for 30 min in 70% ethanol, followed by three times for 30 min in 85% ethanol, and three times for 30 min in 100% ethanol.
 - b. Clearing: Immerse the tissues in a xylene bath three times for 20 min.
 - c. Embed in liquid paraffin at 59°C.
- Note: These steps can be performed by an automated instrument like the "Tissue-Tek-VIP."*
3. Cut 4- μ m-thick tissue sections using a rotary microtome and place on Superfrost slides.

B. Removal of paraffin

1. Rinse the slides in Neo Clear twice for 10 min.
2. Place the slides in a 100% ethanol bath for 5 min.
3. Place the slides in a 96% ethanol bath for 5 min.
4. Place the slides in an 80% ethanol bath for 5 min.
5. Place the slides in a 70% ethanol bath for 5 min.
6. Place the slides in a 50% ethanol bath for 5 min.
7. Rinse in ultrapure distilled water three times for one minute.
8. Rinse in 1 \times PBS.

C. Antigen retrieval

1. Place the slides in a vertical, plastic staining rack and add antigen retrieval buffer to totally

immerse the paraffin-embedded samples (around 50 ml buffer for an 8-slide rack).

2. Fill the sterilizer with an adequate amount of distilled water.
3. Place the rack in the sterilizer and close it.
4. Allow the sterilizer to heat to 120-135°C, and incubate for 10-15 min.
5. After 10-15 min, open the lid and allow the slides to cool to RT on the bench for approximately 20 min.
6. Rinse twice with 1× PBS.

D. Permeabilization

1. Immerse the slides in permeabilization buffer for 2 min.
2. Rinse twice with 1× PBS.

E. Blocking

1. Place the slides in the staining rack and incubate with blocking buffer for one hour at RT.
2. Keep the excess blocking buffer at 4°C.
3. During the blocking step, prepare the StainTray slide staining system. Place moistened paper in the tray.
4. Rinse the slides once with 1× PBS.

F. Primary staining

1. Prepare the primary staining mix. Use 80 µl staining mix for every 1 cm² of sample. Adapt the quantity of staining mix according to the surface area of the sample. Add goat anti-MPO at a 1/40 dilution and rabbit anti-histone 3 at a 1/100 dilution in blocking buffer.
2. Place the slides in the staining system tray.
3. Place the staining mix on the tissue sections to completely immerse them.
4. Close the staining system and incubate at RT for one hour.
5. Transfer the slides to a plastic rack.
6. Rinse three times with 1× PBS.

G. Secondary staining

1. Prepare the secondary staining mix. Add anti-goat Alexa Fluor 488 at a 1/200 dilution, anti-rabbit Alexa Fluor 568 at a 1/200 dilution, and DAPI at a 1/1,000 dilution in blocking buffer.
2. Place the slides in the staining system tray.
3. Place the staining mix on the tissue sections to completely immerse them.
4. Close the staining system and incubate for two hours at RT.
5. Transfer the slides to a plastic rack.
6. Rinse three times with 1× PBS.
7. Remove the moistened paper from the staining system tray.
8. Dry the slides.

Important: *Never touch the tissue sections.*

9. From this point onward, work in a chemical fume hood to allow for optimal drying. Place a drop of ProLong Gold onto the tissue sections and add a coverslip. Allow the slides to dry overnight, protected from the light, but without totally closing the staining system to facilitate air circulation. In some experiments using other mounting media, we observed a rapid loss of the Cit-H3 staining. Since ProLong Gold is described to protect fluorescent dyes from fading and photobleaching, we chose this mounting medium.
10. Analyze the slides and acquire images using a confocal microscope within two days of staining.

H. Controls

You can perform two types of negative control. You can perform primary staining with isotype control antibodies, *i.e.*, goat IgG and rabbit IgG isotype control antibodies instead of anti-MPO and anti-citrullinated Histone 3, at similar concentrations. Alternatively, you can replace the primary staining with an incubation with sera from the host species in which the primary antibodies were produced (*i.e.*, rabbit and goat serum). In both cases, the secondary staining remains the same.

Data analysis

A. Image acquisition

Images are acquired using a confocal microscope (here, a Zeiss LSM 880). Select the appropriate lasers; in this case, 488 nm (MPO), 561 nm (Cit-H3), and 405 nm (DAPI). Adjust the laser voltages to identify stained structures. To ensure the specificity of your staining, compare positive samples with control samples. Once the lasers have been set up, be sure to always use the same settings for all the slides that you want to analyze and compare. NETs are identified as extracellular structures that stain positive for MPO and Cit-H3. DAPI staining is not always observed in NETs, as NETs are composed of decondensed chromatin (Figure 1). To further quantitate the NETs, we performed Z-stack acquisition of 6-10 random fields on each section at 20× magnification.

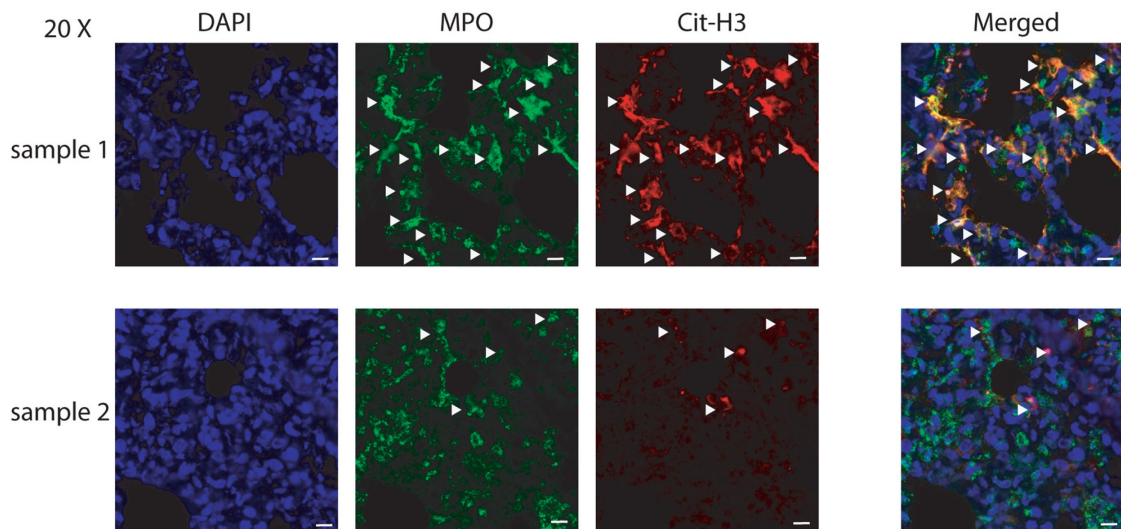


Figure 1. Representative images of lung NETs. NETs are identified as extracellular structures where MPO (AF-488, green) and Cit-H3 (AF568, red) co-localize (shown by white arrows). Co-localization with DAPI could not always be observed. Images were acquired at 20× magnification. Scale bars, 10 μm .

B. Quantitation of NET volume

To quantitate NETs in lung tissue sections (Figure 2), we analyzed 6-10 (20× magnification) per section, and one section per patient (Radermecker *et al.*, 2020). We acquired Z-stack images using the Imaris software. We performed a three-dimensional reconstruction of structures that stained double-positive for Cit-H3 (red) and MPO (green) (Figure 2), and Imaris provided quantitation of the volume of these structures. The co-localization method uses three Imaris script/macro tools (Table 1). The first script processes all the .ims files in a folder, then thresholds the red Cit-H3 and green MPO staining. During this step, we used a threshold to separate voxels from background, and voxels from staining, in each separate channel. We defined true staining as all the staining above 10 voxels. Then, the thresholding method replaced each pixel in an image with a black pixel, if the image intensity was less than the threshold previously fixed (10 voxels), or a white pixel, if the image intensity was greater than that threshold. Subsequently, we created a new channel, *i.e.*, the intersection between the red and green thresholds, where all the voxels have a co-localization equal to 1. The second script then measured the volume of the intersection between the red and green thresholds. Finally, the third script measured the total volume of the image and created an Excel .xlsx file containing all the measurements. Finally, we divided the volume obtained (volume of the intersection of red and green channels) by the total volume of lung tissue analyzed in each sample to yield the cubic micrometers of NETs per cubic micrometer of lung tissue. All the procedures for quantitation are represented in Figure 3.

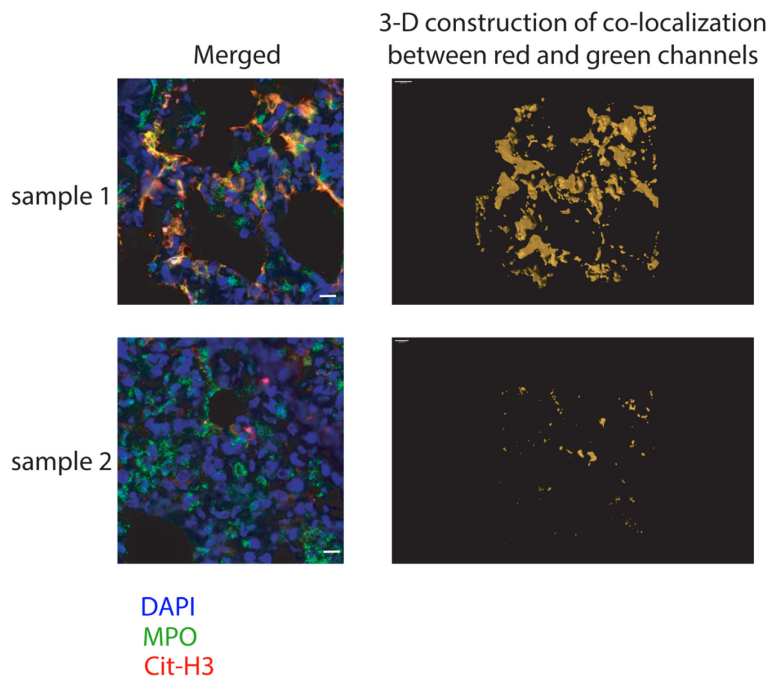


Figure 2. Example of a 3D construction of volumes, where co-localization of MPO and Cit-H3 is present. Confocal microscopy staining (left) and three-dimensional modeling (right) of Cit-H3+MPO+ NETs. Scale bars, 10 μ m.

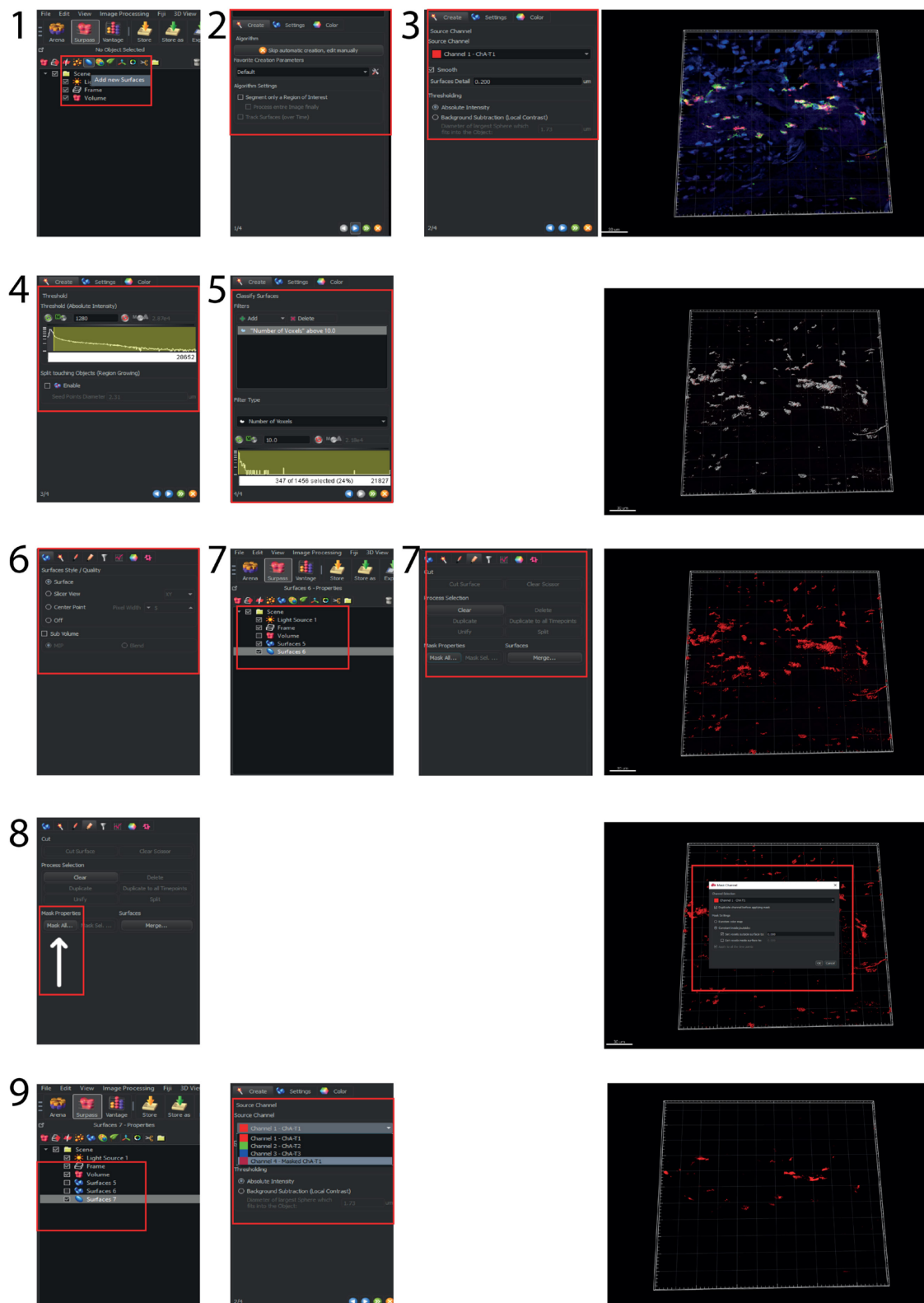


Figure 3. Procedure for the 3D reconstruction of volumes, where co-localization of MPO and Cit-H3 is present on Imaparis. 1) Add a new red surface; 2) Initiate; 3) Choose the red channel, smooth 0.2, absolute intensity; 4) Set the threshold to 1280; 5) Classify the surface above 10; 6) Validate the surface; 7) Repeat steps 2-6 with the green channel; 8) Select channel green > cut >

Mask all > Channel 1 and duplicate the channel before applying mask > constant outside to 0; 9)
Repeat steps 2-6 with Mask of red channel.

Table 1. Scripts used for the quantitation of NET volume

Green algorithm	Red algorithm
Enable Region Of Interest = false	Enable Region Of Interest = false
Enable Region Growing = false	Enable Region Growing = false
Enable Tracking = false	Enable Tracking = false
[Source Channel]	[Source Channel]
Source Channel Index = 4	Source Channel Index = 1
Enable Smooth = true	Enable Smooth = true
Surface Grain Size = 0.200 μm	Surface Grain Size = 0.200 μm
Enable Eliminate Background = false	Enable Eliminate Background = false
Diameter Of Largest Sphere = 1.00 μm	Diameter Of Largest Sphere = 1.00 μm
[Threshold]	[Threshold]
Enable Automatic Threshold = false	Enable Automatic Threshold = false
Manual Threshold Value = 1200	Manual Threshold Value = 1030
Active Threshold = true	Active Threshold = true
Enable Automatic Threshold B = true	Enable Automatic Threshold B = true
Manual Threshold Value B = 10964.9	Manual Threshold Value B = 6835.53
Active Threshold B = false	Active Threshold B = false
[Classify Surfaces]	[Classify Surfaces]
"Number of Voxels" above 10.0	"Number of Voxels" above 10.0

C. Statistical analysis

We represented the data as the mean for each section and analyzed it for statistical significance using a non-parametric Mann-Whitney U test on the mean values. *P* values < 0.05 were considered statistically significant.

Notes

1. While the current protocol has been mainly employed in human lung formalin-fixed paraffin-embedded (FFPE) sections, it has also been applied to human liver, pancreas, kidney, and heart FFPE sections (Radermecker *et al.*, 2020). While we did not detect NET structures in those organs of severe Covid-19 patients, neither did we detect non-specific staining, suggesting that the protocol could also be applied to these organs.
2. Of note, MPO can also be expressed by other phagocytes, such as human macrophages or eosinophils, which may also form extracellular traps and stain for Cit-H3; therefore, the present

protocol would be more specific for neutrophils and NETs if an additional stain directed against a neutrophil marker, such as Ly-6G, was used. From our experience, anti-Ly-6G antibodies do not work properly on FFPE sections, and some clones also detect Ly-6C, which does not help to solve the specificity issue. In laboratory mice, selective depletion of neutrophils, such as an anti-Ly-6G-mediated depletion, can be used to confirm the specificity of the method, as performed previously (Radermecker *et al.*, 2019). Indeed, NETs were shown to be present in lungs from neutrophil-sufficient mice exposed intranasally to a low dose of lipopolysaccharide, but NETs were absent in neutrophil-depleted mice (Radermecker *et al.*, 2019).

Recipes

1. Antigen Retrieval Buffer

Make a 1/10 dilution of HIER Tris-EDTA Buffer pH 9.0 (10×) in distilled water. Add Tween-20 at a final concentration of 0.05%.

2. Permeabilization Buffer

Add Triton X-100 to PBS at a final concentration of 0.5%.

3. Blocking Buffer

Add BSA at a final concentration of 2% and donkey serum at a final concentration of 2% in PBS.

Acknowledgments

The immunofluorescence protocol was adapted from an article by Toussaint and colleagues (Toussaint *et al.*, 2017). The quantitation method is described in Radermecker *et al.* (2019 and 2020).

Competing interests

The authors declare no competing interests.

Ethics

The use of human specimens was approved in 2020 by the Ethics Review Board of the University Hospital of Liege (ref 2020/119).

References

1. Borregaard, N. (2010). [Neutrophils, from marrow to microbes](#). *Immunity* 33(5): 657-670.
2. Brinkmann, V., Reichard, U., Goosmann, C., Fauler, B., Uhlemann, Y., Weiss, D. S., Weinrauch, Y. and Zychlinsky, A. (2004). [Neutrophil extracellular traps kill bacteria](#). *Science* 303(5663): 1532-1535.

3. Caldarone, L., Mariscal, A., Sage, A., Khan, M., Juvet, S., Martinu, T., Zamel, R., Cypel, M., Liu, M., Palaniyar, N. and Keshavjee, S. (2019). [Neutrophil extracellular traps in ex vivo lung perfusion perfusate predict the clinical outcome of lung transplant recipients](#). *Eur Respir J* 53(4).
4. Caudrillier, A., Kessenbrock, K., Gilliss, B. M., Nguyen, J. X., Marques, M. B., Monestier, M., Toy, P., Werb, Z. and Looney, M. R. (2012). [Platelets induce neutrophil extracellular traps in transfusion-related acute lung injury](#). *J Clin Invest* 122(7): 2661-2671.
5. Hakkim, A., Furnrohr, B. G., Amann, K., Laube, B., Abed, U. A., Brinkmann, V., Herrmann, M., Voll, R. E. and Zychlinsky, A. (2010). [Impairment of neutrophil extracellular trap degradation is associated with lupus nephritis](#). *Proc Natl Acad Sci U S A* 107(21): 9813-9818.
6. Hidalgo, A., Chilvers, E. R., Summers, C. and Koenderman, L. (2019). [The Neutrophil Life Cycle](#). *Trends Immunol* 40(7): 584-597.
7. Liu, S., Su, X., Pan, P., Zhang, L., Hu, Y., Tan, H., Wu, D., Liu, B., Li, H., Li, H., Li, Y., Dai, M., Li, Y., Hu, C. and Tsung, A. (2016). [Neutrophil extracellular traps are indirectly triggered by lipopolysaccharide and contribute to acute lung injury](#). *Sci Rep* 6: 37252.
8. Mestas, J. and Hughes, C. C. W. (2004). [Of Mice and Not Men: Differences between Mouse and Human Immunology](#). *J Immunol* 172(5): 2731-2738.
9. Middleton, E. A., He, X. Y., Denorme, F., Campbell, R. A., Ng, D., Salvatore, S. P., Mostyka, M., Baxter-Stoltzfus, A., Borczuk, A. C., Loda, M., Cody, M. J., Manne, B. K., Portier, I., Harris, E. S., Petrey, A. C., Beswick, E. J., Caulin, A. F., Iovino, A., Abegglen, L. M., Weyrich, A. S., Rondina, M. T., Egeblad, M., Schiffman, J. D. and Yost, C. C. (2020). [Neutrophil extracellular traps contribute to immunothrombosis in COVID-19 acute respiratory distress syndrome](#). *Blood* 136(10): 1169-1179.
10. Narasaraju, T., Yang, E., Samy, R. P., Ng, H. H., Poh, W. P., Liew, A. A., Phoon, M. C., van Rooijen, N. and Chow, V. T. (2011). [Excessive neutrophils and neutrophil extracellular traps contribute to acute lung injury of influenza pneumonitis](#). *Am J Pathol* 179(1): 199-210.
11. Papayannopoulos, V. (2018). [Neutrophil extracellular traps in immunity and disease](#). *Nat Rev Immunol* 18(2): 134-147.
12. Pillay, J., den Braber, I., Vrisekoop, N., Kwast, L. M., de Boer, R. J., Borghans, J. A., Tesselaar, K. and Koenderman, L. (2010). [In vivo labeling with 2H₂O reveals a human neutrophil lifespan of 5.4 days](#). *Blood* 116(4): 625-627.
13. Radermecker, C., Detrembleur, N., Guiot, J., Cavalier, E., Henket, M., d'Emal, C., Vanwinge, C., Cataldo, D., Oury, C., Delvenne, P. and Marichal, T. (2020). [Neutrophil extracellular traps infiltrate the lung airway, interstitial, and vascular compartments in severe COVID-19](#). *J Exp Med* 217(12).
14. Radermecker, C., Sabatel, C., Vanwinge, C., Ruscitti, C., Maréchal, P., Perin, F., Schyns, J., Rocks, N., Toussaint, M., Cataldo, D., Johnston, S. L., Bureau, F. and Marichal, T. (2019). [Locally instructed CXCR4^{hi} neutrophils trigger environment-driven allergic asthma through the release of neutrophil extracellular traps](#). *Nat Immunol* 20(11):1444-1455.

15. Thålin, C., Daleskog, M., Goransson, S. P., Schatzberg, D., Lasselin, J., Laska, A. C., Kallner, A., Helleday, T., Wallen, H. and Demers, M. (2017). [Validation of an enzyme-linked immunosorbent assay for the quantification of citrullinated histone H3 as a marker for neutrophil extracellular traps in human plasma](#). *Immunol Res* 65(3): 706-712.
16. Toussaint, M., Jackson, D. J., Swieboda, D., Guedan, A., Tsourouktsoglou, T. D., Ching, Y. M., Radermecker, C., Makrinioti, H., Aniscenko, J., Bartlett, N. W., Edwards, M. R., Solari, R., Farnir, F., Papayannopoulos, V., Bureau, F., Marichal, T. and Johnston, S. L. (2017). [Host DNA released by NETosis promotes rhinovirus-induced type-2 allergic asthma exacerbation](#). *Nat Med* 23(6): 681-691.
17. Villanueva, E., Yalavarthi, S., Berthier, C. C., Hodgins, J. B., Khandpur, R., Lin, A. M., Rubin, C. J., Zhao, W., Olsen, S. H., Klinker, M., Shealy, D., Denny, M. F., Plumas, J., Chaperot, L., Kretzler, M., Bruce, A. T. and Kaplan, M. J. (2011). [Netting neutrophils induce endothelial damage, infiltrate tissues, and expose immunostimulatory molecules in systemic lupus erythematosus](#). *J Immunol* 187(1): 538-552.